

SPATIAL ACTIVE NOISE CONTROL WITH THE REMOTE MICROPHONE TECHNIQUE: AN APPROACH WITH A MOVING HIGHER ORDER MICROPHONE

Huiyuan Sun, Jihui Zhang, Thushara Abhayapala, Prasanga Samarasinghe,

Audio & Acoustic Signal Processing Group, The Australian National University, Canberra, Australia
{huiyuan.sun, jihui.zhang, thushara.abhayapala, prasanga.samarasinghe}@anu.edu.au

ABSTRACT

Spatial active noise control (ANC) aims to reduce unwanted acoustic noise over a continuous spatial region by generating an anti-noise field with secondary loudspeakers. Conventionally, spatial ANC is achieved by using complex error microphone arrays such as grid or spherical geometry, which are impractical and obstruct the users to enter the quiet region. Recently, the remote microphone technique has been introduced to spatial ANC systems without using error microphones inside the region of interest. However, this technique still requires an error microphone array during the tuning stage. In this paper, we further improve the remote microphone technique by introducing a spatial sound field recording method with a moving higher order microphone for the noise field recording (tuning stage) as well as secondary channel estimations (control stage). This eliminates the requirement for impractical microphone array geometries, typically required in existing spatial ANC solutions. The experimental data based simulation demonstrates the effectiveness of the proposed method on noise reduction over space with its feasible array design.

Index Terms— Active Noise Control, Spatial ANC, Remote Microphone technique, Wave domain signal processing

1. INTRODUCTION

An active noise control (ANC) system aims to reduce unwanted acoustic noise by generating anti-noise with secondary loudspeakers [1]. A spatial ANC system aims to reduce the unwanted noise inside a continuous region of interest [2]. Potential applications include noise control in cars [3, 4], in-flight [5, 6], through an open window [7] and inside other enclosures [8, 9].

Conventionally, spatial ANC is achieved by a multi-input-multi-output (MIMO) adaptive filtering system [10], where the error microphones are required to be uniformly distributed inside the control region [11]. Later, spherical error microphone arrays are applied to spatial ANC systems with harmonic (cylindrical/spherical) based wave-domain sound field processing [12]. This spherical microphone array surrounding the region of interest is difficult to implement, and blocks the users entering and exiting the region. To overcome this impractical error microphone array, the Remote Microphone (RM) technique [13, 14, 15] has been introduced into the spatial ANC system with the MIMO system [16] and in the wave domain [17]. As a result, noise reduction can be achieved with practical physical error microphones locating away from the region of interest, such that the movement of the users in and out of the region during the noise control is possible.

This work is supported by Australian Research Council (ARC) grant DP180102375.

However, introducing the RM technique to spatial ANC does not fully solve the problem of the impractical error microphone array. A spherical error microphone array, acting as the virtual error microphone array, is still necessary in several steps to set up a spatial ANC system. These steps include the secondary channel estimation for the Fx-LMS (Filtered-x Least Mean Square) adaptive filtering system in the control stage, and the recording of the primary noise-field in the tuning stage of the RM technique. In [18], a method for the secondary channel estimation of a spatial ANC system is developed using a moving higher order microphone (HOM). While the secondary channels within the desired frequency range in the region of interest can be obtained without the usage of an error microphone array, it has not been applied in an ANC system yet.

In this paper, we propose a complete method to achieve ANC over space while avoiding the usage of any impractical error microphone arrays. The proposed method is developed based on the wave domain spatial ANC system with the RM technique, while the virtual error microphone array is replaced by a moving HOM. We detail the algorithm of a spatial ANC system with a moving HOM, and analyze the accuracy of the moving HOM recording with experimental results. We compare the noise reduction performance of the proposed method to the conventional spatial ANC system with the RM technique by simulation, and illustrate that the proposed method achieves satisfying performance with a feasible array geometry.

2. PROBLEM FORMULATION

Consider a source-free region of interest Ω in 3D space, where noise sources are outside of Ω . The block diagram of an adaptive feed-forward Fx-LMS filtering ANC system with the wave domain RM method is shown in Fig.1.

In the tuning stage, a group of filters \tilde{C} is estimated in the wave domain to compensate the difference between the primary noise at the virtual microphones d_v and the primary noise at the physical microphones d_p . Note that d_v and d_p is given by the reference noise signal \mathcal{N} filtered by the virtual primary path P_v and the physical primary path P_p , respectively. To estimate the wave domain filter \tilde{C} , Q microphones are uniformly distributed on the sphere of Ω for the spherical harmonic decomposition of the input signals, which refers to the block ‘SH’ in Fig. 1. Hence, we have [19]:

$$\tilde{d}_v^{nm}(k) \approx \frac{1}{j_n(kR)} \sum_{q=1}^Q d_v(r_q, \theta_q, \phi_q, k) Y_{nm}^*(\theta_q, \phi_q) w(q), \quad (1)$$

where $\tilde{d}_v^{nm}(k)$ are the location independent spherical harmonic coefficients with respects to the origin (centre of the region of interest) representing the noise field inside Ω , order n and mode m are integers, $d_v(r_q, \theta_q, \phi_q, k)$ is the recorded noise at the q -th microphone, $k = 2\pi f/c$ is the wave number, f is frequency, c is the speed of

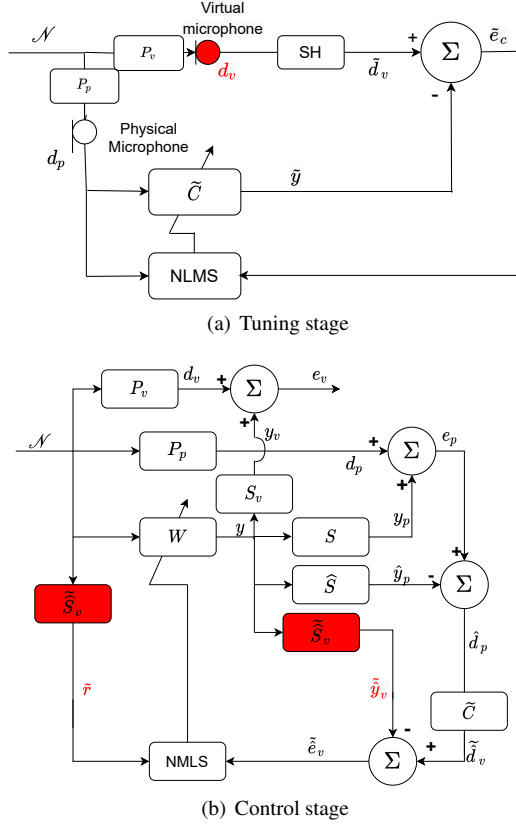


Fig. 1. Block diagram of an adaptive feed-forward spatial ANC system with the wave domain remote microphone technique, to minimize the error signals at e_v from the signals recorded at physical microphones e_p .

sound, $j_n(\cdot)$ is the spherical Bessel function, $Y_{nm}(\cdot)$ is the spherical harmonic function [20], and $w(q)$ is the sampling weight of the q -th microphone. At least $Q \geq ([kR] + 1)^2$ virtual microphones are necessary, where R is the radius of Ω . Hereafter, we use (\cdot) to represent that a variable is given in the wave domain by spherical harmonic coefficients, use (\cdot) to represent the estimation value of a variable, and omit the frequency component k for simplicity.

In the control stage (Fig. 1(b)), we record the sound pressure values at the physical microphone locations as e_p without microphones at the virtual microphone locations. e_p is the summation of the primary noise $d_p = \mathcal{N}P_p$ and the secondary sound $y_p = yS$, where y is the driving signals of the secondary loudspeaker array given by $y = \mathcal{N}W$, S is the matrix of physical secondary channels. The estimated residual sound field coefficients of the region of interest \tilde{e}_v is hence given by [17]

$$\tilde{e}_v = \tilde{d}_v + \mathcal{N}W\tilde{S}_v = \tilde{C}e_p - \tilde{C}\mathcal{N}W\hat{S} + \mathcal{N}W\tilde{S}_v. \quad (2)$$

where \tilde{d}_v is the estimated primary noise field coefficients in the region of interest, \mathcal{N} is the reference noise signal, $W = [w_1, w_2, \dots, w_L]^T$ is a group of adaptive filter weights for the driving signals of the secondary loudspeakers, \hat{S} is the estimation of the secondary channels of the physical microphones, and \tilde{S}_v is the estimation of the secondary channel coefficients of the virtual microphones.

Define the cost function of the adaptive filter as

$$\xi(t) = \tilde{e}_v \tilde{e}_v^H, \quad (3)$$

where $(\cdot)^H$ refers to the conjugate transpose of a matrix. We can get the update equation of the wave domain spatial ANC with the RM technique as

$$w_\ell(t+1) = w_\ell(t) - \lambda \mathcal{N} \tilde{e}_v \tilde{S}_v^H, \quad (4)$$

where λ is the step size.

With the RM technique, \tilde{e}_v has been minimized with the absence of a spherical virtual error microphone array in the control stage. However, two blocks in Fig. 1 still require the recording from the virtual microphone array (colored red): the recording of the primary noise field coefficients in the tuning stage, and the pre-measure of the virtual secondary channels in the control stage.

In [18], the secondary channel estimation has been achieved using a moving HOM instead of a spherical microphone array. The error microphone array is first replaced by a number of distributed HOMs to achieve the same sound field coefficients recording. Then, these HOMs are further replaced by a single moving HOM at a cost of roughly 10 dB SNR based on a simulation study.

Consider Q microphones with arbitrary directivities given by $G_1(\theta_1, \phi_1), \dots, G_Q(\theta_Q, \phi_Q)$, and with an arbitrary geometry within a certain region at $\mathbf{x}_1, \dots, \mathbf{x}_Q$, respectively. The signal recorded at the q -th microphone at $\mathbf{x}_q = (r_q, \theta_q, \phi_q)$ is given by [21]

$$p_q = \tilde{\mathbf{g}}_q^H \tilde{\mathbf{p}}_q = \tilde{\mathbf{g}}_q^H \mathbf{T}(\mathbf{x}_q - \mathbf{x}_0) \tilde{\mathbf{p}}_0, \quad (5)$$

where $\tilde{\mathbf{g}}_q$ is the vector of spherical harmonic coefficients of the q -th microphone's directivity $G_q(\theta_q, \phi_q)$, $\tilde{\mathbf{p}}_0$ is the vector of spherical harmonic coefficients at \mathbf{x}_0 , which refers to the origin, $\mathbf{T}(\mathbf{x}_q - \mathbf{x}_0)$ is the translation matrix, with each element as [22]

$$\begin{aligned} T_{n\nu}^{m\mu}(\mathbf{x}, k) = & 4\pi i^{\nu-n} \sum_{\ell=0}^{\infty} i^\ell (-1)^{2m-\mu} \\ & \times \sqrt{\frac{(2n+1)(2\nu+1)(2\ell+1)}{4\pi}} \\ & \times j_\ell(kr) Y_{\ell(\mu-m)}^*(\theta, \phi) W_1 W_2, \end{aligned} \quad (6)$$

where order ν , mode μ , and ℓ are integers, and W_1 and W_2 refer to the Wigner $3-j$ symbol [23].

Based on the sound-field translation technique introduced in [21], the spherical harmonic coefficients with respects to an arbitrary point \mathbf{x} in the region of interest is given by

$$\tilde{\mathbf{p}}_{\mathbf{x}} = \Xi(\mathbf{x})(\Psi + \sigma^{-2}\Sigma)^{-1} \mathbf{p}, \quad (7)$$

where $\Xi(\mathbf{x}_0) = [\mathbf{T}(\mathbf{x}_0 - \mathbf{x}_1)g_1, \dots, \mathbf{T}(\mathbf{x}_0 - \mathbf{x}_Q)g_Q]$, $\Xi(\mathbf{x}) = \mathbf{T}(\mathbf{x} - \mathbf{x}_0)\Xi(\mathbf{x}_0)$, $\sigma^{-2}\Sigma$ is the noise covariance Σ to the average signal power (σ^2) ratio which can be treated as the regularization parameter of the microphone's noise, $\mathbf{p} = [p_1, p_2, \dots, p_Q]$ is the vector of the recorded sound pressure by Q microphones, and Ψ is a matrix with the element at the q -th column and the q' -th row as

$$\Psi_{(q,q')} = \tilde{\mathbf{g}}_q^H \mathbf{T}(\mathbf{x}_q - \mathbf{x}_{q'}) \tilde{\mathbf{g}}_{q'}. \quad (8)$$

In this way, the spherical harmonic coefficients of a sound field can be obtained by Q distributed HOMs in the region within the desired frequency range. Thus, we can obtain the frequency response (secondary channel) at any desired point in the region.

In this paper, we introduce a similar method of sound field recording with distributed HOMs into the wave domain ANC system with the RM technique. Specifically, we apply this method in the tuning stage filter \tilde{C} calculation. In section 3, we introduce the new tuning stage with the distributed HOMs. In section 4, we analysis the influence of having a moving HOM replacing the fix-positioned HOMs by using experimental data.

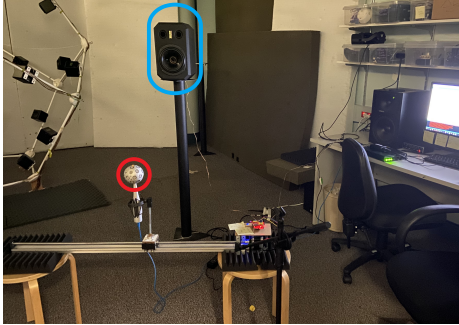


Fig. 2. The proposed setup for recording the sound field generated from a loudspeaker (blue) using a moving Eigenmike (red).

3. DISTRIBUTED HIGHER ORDER MICROPHONES IN THE TUNING STAGE OF THE RM TECHNIQUE

According to (7), by using Q distributed HOMs in the region of interest, we are able to obtain the noise field at any point inside the region, including the desired primary noise d_v at the virtual microphone positions.

However, we can not achieve a real-time tuning stage recording as described in Fig.1(a). This is because we can not record the primary noise field at the virtual microphones and at the physical error microphones simultaneously with the distributed/moving HOMs. The RM technique generally only works with a stationary noise field [24]. With this assumption of stationary noise field in hands, we are able to record the physical primary noise field and the virtual noise field separately. Hence, the required filter \tilde{C} can be calculated by

$$\tilde{C} = d_p^\dagger \tilde{d}_v, \quad (9)$$

where $(\cdot)^\dagger$ refers to the Moore-Penrose inverse, d_p is given by direct measurements, and \tilde{d}_v is calculated by (7) from the HOMs recording. Hence, in the control stage, the estimated residual sound field coefficients of the region of interest \tilde{e}_v is given by [17]

$$\tilde{e}_v = \tilde{C} e_p - \tilde{C} \mathcal{N} W \hat{S} + \mathcal{N} W \tilde{\hat{S}}_v. \quad (10)$$

In this way, we achieve a spatial ANC system with the virtual microphone array to be replaced by distributed HOMs. In the next section, we examine the impacts of further replacing these distributed HOMs by a single moving HOM with a constant speed.

4. INFLUENCE OF A MOVING HOM

In the previous sections, we detail the method of using distributed HOMs to replace the impractical error microphone array in a spatial ANC system. However, HOM array is difficult and extremely costly to implement. In [18], the possibility of replacing the HOM array with a single moving HOM is preliminarily investigated. In this section, we further verify the effectiveness of this idea by experiments.

We constructed an experiment with a commercially available 4-th order microphone, (Eigenmike [25]), a loudspeaker and a mechanical slide rail in a lab-room at the Australian National University with the dimension of [3.6, 6.7, 2.8] m. Figure 2 shows the experiment setup, where the Eigenmike and the loudspeaker were circled in red and blue, respectively. A 12-th order maximum length sequence signal was used as the driving signal of the loudspeaker.

To test the error between a moving Eigenmike recording and a fixed positioned Eigenmike recording, we first recorded the sound field with the Eigenmike at the start point as the reference. Then,

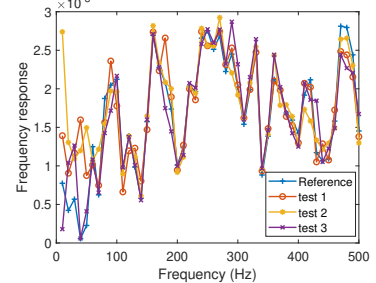


Fig. 3. Frequency response of one microphone on the fixed positioned Eigenmike (reference) and moving Eigenmikes (test 1-3).

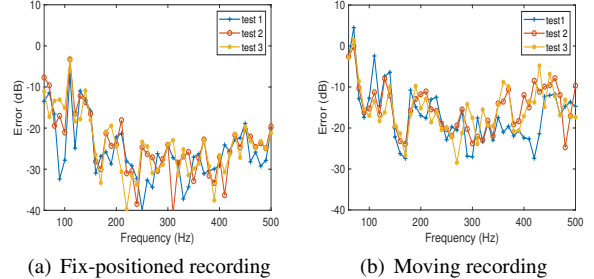


Fig. 4. Average error of frequency response recording over 32 channels on a Eigenmike with (a) fix positioned Eigenmike, and (b) moving Eigenmike for 3 repeated experiment, respectively.

we controlled a stepper motor with a micro-processor to move the Eigenmike with a constant speed of approximately 1 cm/s, and recorded the same sound field. We repeated the recording with moving Eigenmike for several times. The position of the Eigenmike was moved back to the start point after each test.

Figure 3 shows the frequency response of one channel on the Eigenmike with the frequency range of [0, 500] Hz, which is the desired frequency range of a typical ANC. A recording with fix-positioned Eigenmike was used as reference. Test 1-3 was given by the recording of the moving Eigenmike, respectively. We can observe from Fig.3 that the moving Eigenmike can achieve similar frequency response recording as the fixed positioned Eigenmike within the desired frequency range. The error at lower frequency range (below 50 Hz) is high. This may be due to the non-stationary noise in the environment.

We examined the average error over all 32 channels on the Eigenmike in Fig.4. We used the first fix-positioned recording as the reference, and examined the error of three repeated recording from fix-positioned Eigenmike in Fig.4(a) and three repeated recording from moving Eigenmike in Fig.4(b). It is shown in Fig.4 that the recordings of the moving Eigenmike have higher error than the fix-positioned Eigenmike, as expected. The difference of the average error over three experiments between the fix-positioned Eigenmike and the moving Eigenmike is given in Fig. 5.

From this experimental result, we concluded that on average 10dB noise is introduced into the recording within the desired frequency range by a moving HOM recording. Hence, in the following simulation of the spatial ANC system, we assume the physical error microphones (fixed-position) to have 40 dB SNR, and 30dB SNR on the error microphones at virtual positions to mimic a moving HOM.

5. SIMULATION AND RESULTS

In this section, we first evaluate the noise reduction performance of the proposed spatial ANC method over the x-y and x-z planes. Then,

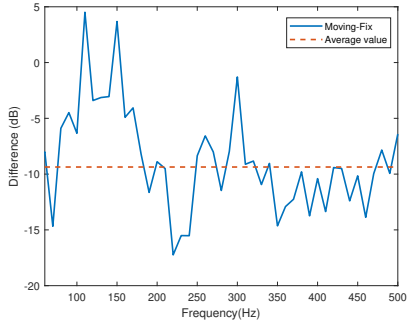


Fig. 5. The difference of the average error over 3 repeated experiments between the fix-positioned Eigenmike and the moving Eigenmike and its average value over the desired frequency band.

we compare its overall noise reduction performance over the region of interest against the existing method for spatial ANC with the RM technique [17].

To control the noise below 500 Hz, a 4-th order system is constructed with a region of interest of the radius $r = 0.3$ m. We test the system in a room environment with $5\text{ m} \times 6\text{ m} \times 4\text{ m}$ in size and with 0.8 of wall reflection coefficients. The room environment is simulated by the image source method [26]. The noise source is located at $(1.5, 1.7, 0.5)$ m, with a reference microphone nearby¹. 32 loudspeakers evenly distributed on the surface of a sphere with radius $R = 1.5$ m is applied as secondary loudspeakers. We use 8 physical microphones at 8 corners of a 0.8 m side length cubic enclosing the region of interest.

In the existing RM based spatial ANC solution [17], the same scenario requires 32 error microphones uniformly distributed on the surface of the region of interest as the virtual microphone array. In the proposed method, this virtual microphone array can be replaced by a moving Eigenmike for virtual secondary channel estimations prior to the control stage and primary noise field recordings in the tuning stage, according to Sec.2 and Sec. 3. However, given the lack of efficient simulation method for a moving microphone's recording, we use the results form Sec. 4, and mimic the moving Eigenmike with 9 fixed-positioned Eigenmikes uniformly distributed on the surface of the region with a higher measurement noise. Although in total we use more microphones in the proposed method, we avoid the usage of a 0.3 m radius spherical microphone array, which is impractical to construct.

Figure 6 shows the sound field over the x-y plane and the x-z plane of the original noise field, and the residual noise field after noise reduction by the proposed method, respectively. A single tone sine wave of 375 Hz is applied as the noise signal. The region of interest is marked by a white circle. We observe that the proposed method successfully reduces the residual noise energy inside the region of interest.

In Fig. 7, we show the average noise reduction performance over the region of interest against time (iterations) by the proposed method and the conventional method. We define the average noise reduction performance as

$$\eta(k) = 10 \log_{10} \frac{\sum_{\mathbf{x}} E\{|e(\mathbf{x}, k)|^2\}}{\sum_{\mathbf{x}} E\{|d(\mathbf{x}, k)|^2\}}, \quad (11)$$

where $e(\mathbf{x}, k)$ is the residual noise pressure at point $\mathbf{x} \in \Omega$ and $d(\mathbf{x}, k)$ is the original noise without ANC. We observe that the pro-

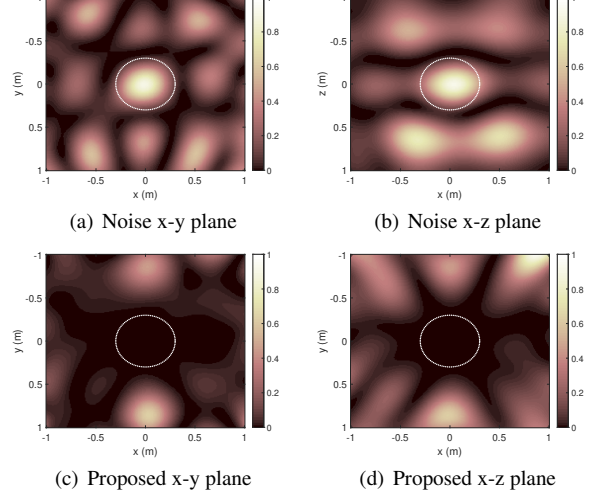


Fig. 6. Noise field over (a) the x-y plane and (b) the x-z plane of the original noise field; the residual noise field after noise reduction by the proposed method over (c) the x-y plane and (d) the x-z plane.

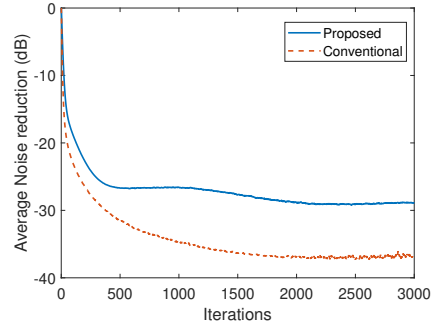


Fig. 7. Average noise reduction performance in the region with the proposed method and the conventional method over iterations.

posed method achieves an average more than 25 dB noise reduction over the region after convergence. Comparing to the conventional method with the proper virtual error microphone array, the noise reduction performance of the proposed method decreases. However, we consider this performance difference is not significant comparing with the more than 25 dB noise reduction. This sacrifice on performance results in a more practical microphone geometry, which makes the spatial ANC system much more feasible in the real world.

6. CONCLUSION

In this paper, we address a wave-domain spatial ANC system with RM technique without the usage of virtual error microphone array. The impractical virtual error microphone array, which is necessary in the conventional spatial ANC system, is replaced by distributed HOMs. By experiments, we demonstrate that the usage of these distributed HOMs can be further optimized by using a single moving HOM with a tolerable error. By simulation, we show that the proposed method with a single moving HOM provides a satisfying noise reduction performance. Hence, we consider the proposed method with a single moving HOM to have more realistic array geometry, which is a step forward in realizing spatial ANC for real-world applications. The experimental implementation of a spatial ANC system with the proposed method will be provided in the future work.

¹The controlling of the feedback signal from the secondary loudspeakers is out of the scope of this paper.

7. REFERENCES

- [1] C. C. Fuller, S. Elliott, and P. A. Nelson, *Active control of vibration*, Academic Press, 1996.
- [2] Y. Kajikawa, W. S. Gan, and S. M. Kuo, "Recent advances on active noise control: open issues and innovative applications," *APSIPA Transactions on Signal and Information Processing*, vol. 1, pp. 21, Aug. 2012.
- [3] H. Sano, T. Inoue, A. Takahashi, K. Terai, and Y. Nakamura, "Active control system for low-frequency road noise combined with an audio system," *IEEE Transactions on speech and audio processing*, vol. 9, no. 7, pp. 755–763, 2001.
- [4] W. Jung, S. J. Elliott, and J. Cheer, "Local active control of road noise inside a vehicle," *Mechanical Systems and Signal Processing*, vol. 121, pp. 144–157, 2019.
- [5] S. J. Elliot, P. A. Nelson, I. M. Stothers, and C. C. Boucher, "In-flight experiments on the active control of propeller-induced cabin noise," *Journal of Sound and Vibration*, vol. 140, no. 2, pp. 219–238, 1990.
- [6] T. Haase, O. Unruh, S. Algermissen, and M. Pohl, "Active control of counter-rotating open rotor interior noise in a dornier 728 experimental aircraft," *Journal of Sound and Vibration*, vol. 376, pp. 18–32, 2016.
- [7] T. Murao, C. Shi, W. S. Gan, and M. Nishimura, "Mixed-error approach for multi-channel active noise control of open windows," *Applied Acoustics*, vol. 127, pp. 305–315, 2017.
- [8] P. Belanger, A. Berry, Y. Pasco, O. Robin, Y. St-Amant, and S. Rajan, "Multi-harmonic active structural acoustic control of a helicopter main transmission noise using the principal component analysis," *Applied Acoustics*, vol. 70, no. 1, pp. 153–164, 2009.
- [9] A. Montazeri and C. J. Taylor, "Modeling and analysis of secondary sources coupling for active sound field reduction in confined spaces," *Mechanical Systems and Signal Processing*, vol. 95, pp. 286–309, Oct. 2017.
- [10] Sen M Kuo and Dennis R Morgan, "Active noise control: a tutorial review," *Proceedings of the IEEE*, vol. 87, no. 6, pp. 943–973, 1999.
- [11] E. G. Williams, *Fourier acoustics: sound radiation and nearfield acoustical holography*, Elsevier, 1999.
- [12] J. Zhang, T. D. Abhayapala, W. Zhang, P. N. Samarasinghe, and S. Jiang, "Active noise control over space: A wave domain approach," *IEEE/ACM Transactions on Audio, Speech, and Language Processing (TASLP)*, vol. 26, no. 4, pp. 774–786, 2018.
- [13] Danielle Moreau, Ben Cazzolato, Anthony Zander, and Cornelis Petersen, "A review of virtual sensing algorithms for active noise control," *Algorithms*, vol. 1, no. 2, pp. 69–99, 2008.
- [14] Alain Roure and Anne Albarrazin, "The remote microphone technique for active noise control," in *INTER-NOISE and NOISE-CON Congress and Conference Proceedings*. Institute of Noise Control Engineering, 1999, vol. 1999, pp. 1233–1244.
- [15] Stephen Elliott, CK Lai, Thibault Vergez, and Jordan Cheer, "Robust stability and performance of local active control systems using virtual sensing," in *23rd International Congress on Acoustics, integrating 4th EAA Euroregio 2019*, 2019.
- [16] Dongyuan Shi, Bhan Lam, and Woon-seng Gan, "Analysis of multichannel virtual sensing active noise control to overcome spatial correlation and causality constraints," in *ICASSP 2019-2019 IEEE International Conference on Acoustics, Speech and Signal Processing (ICASSP)*. IEEE, 2019, pp. 8499–8503.
- [17] Huiyuan Sun, Jihui Zhang, Thushara D Abhayapala, and Prasanga N Samarasinghe, "Active noise control over 3d space with remote microphone technique in the wave domain," in *2021 IEEE Workshop on Applications of Signal Processing to Audio and Acoustics (WASPAA)*.
- [18] H. Sun, N. Murata, J. Zhang, T. Magariyachi, P. Samarasinghe, S. Hayashi, T. D. Abhayapala, and T. Itabashi, "Secondary channel estimation in spatial active noise control systems using a single moving higher order microphone," *Submitted to The Journal of the Acoustical Society of America*, 2021.
- [19] T. D. Abhayapala, D. B. Ward, et al., "Theory and design of high order sound field microphones using spherical microphone array," in *Proc. IEEE International Conference on Acoustics, Speech, and Signal Processing*, 2002, vol. 2, pp. 1949–1952.
- [20] Frank Bowman, *Introduction to Bessel functions*, Courier Corporation, 2012.
- [21] Natsuki Ueno, Shoichi Koyama, and Hiroshi Saruwatari, "Sound field recording using distributed microphones based on harmonic analysis of infinite order," *IEEE Signal Processing Letters*, vol. 25, no. 1, pp. 135–139, 2017.
- [22] Prasanga Samarasinghe, Thushara Abhayapala, and Mark Poldetti, "Wavefield analysis over large areas using distributed higher order microphones," *IEEE/ACM Transactions on Audio, Speech, and Language Processing*, vol. 22, no. 3, pp. 647–658, 2014.
- [23] P.A. Martin, *Multiple scattering: interaction of time-harmonic waves with N obstacles*, Number 107. Cambridge University Press, 2006.
- [24] Reo Maeda and Yoshinobu Kajikawa, "Comparisons of two virtual sensing methods for broadband noise," in *Proceedings of the 23rd International Congress on Acoustics (2019)*, pp. 6883–6890.
- [25] MH Acoustics, "Em32 eigenmike microphone array release notes (v17.0)," 25 Summit Ave, Summit, NJ 07901, USA, 2013.
- [26] P. N. Samarasinghe, T. D. Abhayapala, Y. Lu, H. Chen, and G. Dickins, "Spherical harmonics based generalized image source method for simulating room acoustics," *The Journal of the Acoustical Society of America*, vol. 144, no. 3, pp. 1381–1391, 2018.